

07825

NATIONAL ADVISORY COMMITTEE FOR AERONAUTICS

DTIC
SELECTED
AUG 31 1995
F

REPORT No. 886

SPARK-TIMING CONTROL BASED ON CORRELATION OF MAXIMUM-ECONOMY SPARK TIMING, FLAME-FRONT TRAVEL, AND CYLINDER-PRESSURE RISE

By HARVEY A. COOK, ORVILLE H. HEINICKE
and WILLIAM H. HAYNE



NAVY RESEARCH SECTION
SCIENCE DIVISION
REFERENCE DEPARTMENT
LIBRARY OF CONGRESS

py#66
10/1/47
FILE COPY
NAVY RESEARCH SECTION
SCIENCE DIVISION
LIBRARY OF CONGRESS
TO BE RETURNED

1
SEP 28 1949

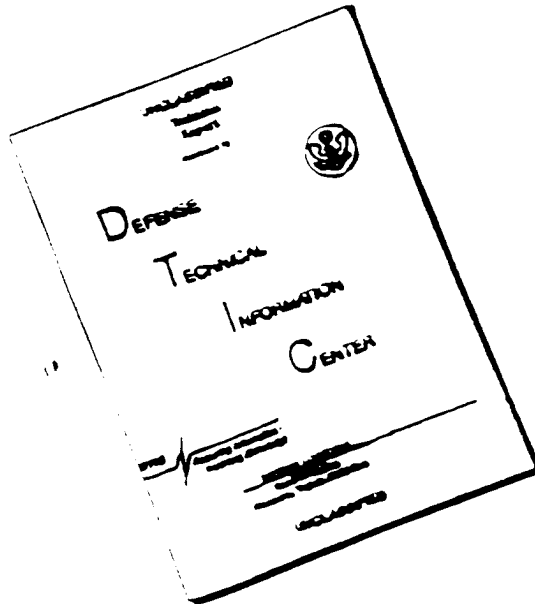
DISTRIBUTION STATEMENT A
Approved for public release
Distribution Unlimited

1947

19950825 132

DTIC QUALITY INSPECTED 5

DISCLAIMER NOTICE



THIS DOCUMENT IS BEST QUALITY AVAILABLE. THE COPY FURNISHED TO DTIC CONTAINED A SIGNIFICANT NUMBER OF PAGES WHICH DO NOT REPRODUCE LEGIBLY.

AERONAUTIC SYMBOLS

1. FUNDAMENTAL AND DERIVED UNITS

	Symbol	Metric		English	
		Unit	Abbreviation	Unit	Abbreviation
Length.....	<i>l</i>	meter.....	m	foot (or mile).....	ft (or mi)
Time.....	<i>t</i>	second.....	s	second (or hour).....	sec (or hr)
Force.....	<i>F</i>	weight of 1 kilogram.....	kg	weight of 1 pound.....	lb
Power.....	<i>P</i>	horsepower (metric).....		horsepower.....	hp
Speed.....	<i>V</i>	kilometers per hour.....	kph	miles per hour.....	mph
		meters per second.....	mps	feet per second.....	fps

2. GENERAL SYMBOLS

<p><i>W</i> Weight = mg</p> <p><i>g</i> Standard acceleration of gravity = 9.80665 m/s^2 or 32.1740 ft/sec^2</p> <p><i>m</i> Mass = $\frac{W}{g}$</p> <p><i>I</i> Moment of inertia = mk^2. (Indicate axis of radius of gyration <i>k</i> by proper subscript.)</p> <p><i>μ</i> Coefficient of viscosity</p>	<p><i>ν</i> Kinematic viscosity</p> <p><i>ρ</i> Density (mass per unit volume)</p> <p>Standard density of dry air, $0.12497 \text{ kg-m}^{-3}\text{-s}^2$ at 15° C and 760 mm; or $0.002378 \text{ lb-ft}^{-3}\text{-sec}^2$</p> <p>Specific weight of "standard" air, 1.2255 kg/m^3 or 0.07651 lb/cu ft</p>
---	---

3. AERODYNAMIC SYMBOLS

<p><i>S</i> Area</p> <p><i>S_w</i> Area of wing</p> <p><i>G</i> Gap</p> <p><i>b</i> Span</p> <p><i>c</i> Chord</p> <p><i>A</i> Aspect ratio, $\frac{b^2}{S}$</p> <p><i>V</i> True air speed</p> <p><i>q</i> Dynamic pressure, $\frac{1}{2}\rho V^2$</p> <p><i>L</i> Lift, absolute coefficient $C_L = \frac{L}{qS}$</p> <p><i>D</i> Drag, absolute coefficient $C_D = \frac{D}{qS}$</p> <p><i>D₀</i> Profile drag, absolute coefficient $C_{D_0} = \frac{D_0}{qS}$</p> <p><i>D_i</i> Induced drag, absolute coefficient $C_{D_i} = \frac{D_i}{qS}$</p> <p><i>D_p</i> Parasite drag, absolute coefficient $C_{D_p} = \frac{D_p}{qS}$</p> <p><i>C</i> Cross-wind force, absolute coefficient $C_C = \frac{C}{qS}$</p>	<p><i>i_w</i> Angle of setting of wings (relative to thrust line)</p> <p><i>i_t</i> Angle of stabilizer setting (relative to thrust line)</p> <p><i>Q</i> Resultant moment</p> <p><i>Ω</i> Resultant angular velocity</p> <p><i>R</i> Reynolds number, $\frac{Vl}{\mu}$ where <i>l</i> is a linear dimension (e.g., for an airfoil of 1.0 ft chord, 100 mph, standard pressure at 15° C, the corresponding Reynolds number is 935,400; or for an airfoil of 1.0 m chord, 100 mps, the corresponding Reynolds number is 6,865,000)</p> <p><i>α</i> Angle of attack</p> <p><i>ε</i> Angle of downwash</p> <p><i>α₀</i> Angle of attack, infinite aspect ratio</p> <p><i>α_i</i> Angle of attack, induced</p> <p><i>α_a</i> Angle of attack, absolute (measured from zero-lift position)</p> <p><i>γ</i> Flight-path angle</p>
--	---

REPORT No. 886

SPARK-TIMING CONTROL BASED ON CORRELATION OF MAXIMUM-ECONOMY SPARK TIMING, FLAME-FRONT TRAVEL, AND CYLINDER-PRESSURE RISE

By HARVEY A. COOK, ORVILLE H. HEINICKE
and WILLIAM H. HAYNIE

Flight Propulsion Research Laboratory
Cleveland, Ohio

Accession For	
NTIS CRA&I	<input checked="" type="checkbox"/>
DTIC TAB	<input type="checkbox"/>
Unannounced	<input type="checkbox"/>
Justification _____	
By _____	
Distribution / _____	
Availability Codes	
Dist	Avail and/or Special
A-1	

I

National Advisory Committee for Aeronautics

Headquarters, 1724 F Street NW, Washington 25, D. C.

Created by act of Congress approved March 3, 1915, for the supervision and direction of the scientific study of the problems of flight (U. S. Code, title 49, sec. 241). Its membership was increased to 15 by act approved March 2, 1929. The members are appointed by the President, and serve as such without compensation.

JEROME C. HUNSAKER, Sc. D., Cambridge, Mass., *Chairman*

ALEXANDER WETMORE, Sc. D., Secretary, Smithsonian Institution, *Vice Chairman*

HON. JOHN R. ALISON, Assistant Secretary of Commerce.

VANNEVAR BUSH, Sc. D., Chairman, Research and Development Board, Department of National Defense.

EDWARD U. CONDON, Ph. D., Director, National Bureau of Standards.

DONALD B. DUNCAN, Vice Admiral, Deputy Chief of Naval Operations (Air).

R. M. HAZEN, B. S., Chief Engineer, Allison Division, General Motors Corp.

WILLIAM LITTLEWOOD, M. E., Vice President, Engineering, American Airlines System.

THEODORE C. LONNQUEST, Rear Admiral, Assistant Chief for Research and Development, Bureau of Aeronautics, Navy Department.

EDWARD M. POWERS, Major General, United States Air Force, Deputy Chief of Staff, Matériel.

ARTHUR E. RAYMOND, M. S., Vice President, Engineering, Douglas Aircraft Co.

FRANCIS W. REICHELDERFER, Sc. D., Chief, United States Weather Bureau.

CARL SPAATZ, General, Chief of Staff, United States Air Force.

ORVILLE WRIGHT, Sc. D., Dayton, Ohio.

THEODORE P. WRIGHT, Sc. D., Administrator of Civil Aeronautics, Department of Commerce.

HUGH L. DRYDEN, Ph. D., *Director of Aeronautical Research*

JOHN F. VICTORY, LL.M., *Executive Secretary*

JOHN W. CROWLEY, JR., B. S., *Associate Director of Aeronautical Research*

E. H. CHAMBERLIN, *Executive Officer*

HENRY J. E. REID, Sc. D., Director, Langley Memorial Aeronautical Laboratory, Langley Field, Va.

SMITH J. DEFRANCE, B. S., Director Ames Aeronautical Laboratory, Moffett Field, Calif.

EDWARD R. SHARP, LL. B., Director, Flight Propulsion Research Laboratory, Cleveland Airport, Cleveland, Ohio

TECHNICAL COMMITTEES

AERODYNAMICS

POWER PLANTS FOR AIRCRAFT

AIRCRAFT CONSTRUCTION

OPERATING PROBLEMS

SELF-PROPELLED GUIDED MISSILES

INDUSTRY CONSULTING

Coordination of Research Needs of Military and Civil Aviation

Preparation of Research Programs

Allocation of Problems

Prevention of Duplication

Consideration of Inventions

LANGLEY MEMORIAL AERONAUTICAL LABORATORY,
Langley Field, Va.

AMES AERONAUTICAL LABORATORY,
Moffett Field, Calif.

FLIGHT PROPULSION RESEARCH LABORATORY,
Cleveland Airport, Cleveland, Ohio

Conduct, under unified control, for all agencies, of scientific research on the fundamental problems of flight

OFFICE OF AERONAUTICAL INTELLIGENCE,
Washington, D. C.

Collection, classification, compilation, and dissemination of scientific and technical information on aeronautics

REPORT No. 886

SPARK-TIMING CONTROL BASED ON CORRELATION OF MAXIMUM-ECONOMY SPARK TIMING, FLAME-FRONT TRAVEL, AND CYLINDER-PRESSURE RISE

By HARVEY A. COOK, ORVILLE H. HEINICKE, and WILLIAM H. HAYNIE

SUMMARY

An investigation was conducted on a full-scale air-cooled cylinder in order to establish an effective means of maintaining maximum-economy spark timing with varying engine operating conditions. Variable fuel-air-ratio runs were conducted in which relations were determined between the spark timing and the basic factors in engine operation, flame-front travel, and cylinder-pressure rise.

Data obtained in this investigation showed that maximum-economy spark timing occurred when the crank angle of maximum rate of pressure rise was 3° A. T. C. and that the crank angle of maximum rate of pressure rise and travel of the flame front were directly related. For fuel-air ratios between 0.06 and 0.10, the highest rate of flame travel occurred when the crank angle of maximum rate of pressure rise was 3° A. T. C. The previously mentioned relations are significant in fuel or engine investigations in which engine operating variables affect the spark timing for maximum fuel economy.

An instrument for controlling spark timing was developed that automatically maintained maximum-economy spark timing with varying engine operating conditions. The instrument also indicated the occurrence of preignition.

INTRODUCTION

The main factors that are considered in the selection of the spark timing for an engine are fuel economy and knock-limited performance. The maximum fuel-economy spark timing becomes relatively more significant when the knock-limited performance of the fuel is increased. Engines with a fixed spark timing are often operated under conditions where a more advanced spark timing would give a considerable improvement in fuel economy. For this reason, means of varying the spark timing are sometimes used but even then the selection of the best spark timing with varying engine operating conditions is a problem.

In this investigation conducted at the NACA Cleveland laboratory in 1946-47, relations between the spark timing and the basic factors in engine operation (flame-front travel and cylinder-pressure rise) were determined in order to establish an effective means of maintaining maximum-economy spark timing with varying engine operating conditions.

The application of the findings in this investigation affords a convenient means of automatically maintaining maximum-

economy spark timing with varying engine operating conditions. An automatic spark-timing-control instrument is described in the appendix.

APPARATUS AND PROCEDURE

A full-scale air-cooled cylinder was used in the CUE setup described in reference 1. The crank angle of maximum rate of pressure rise θ_r was measured on a diagram of time and rate of pressure change produced on an oscilloscope by the signal from a magnetostriction knock pickup in the cylinder head. Timing marks were produced on the oscilloscope by means of electric impulses generated in a pair of coils mounted on a carriage near the flywheel. The coils had a common magnetic circuit comprised of soft iron cores, a permanent magnet, and an air gap. Steel lugs projecting from the periphery of the flywheel passed through the air gap. The carriage for mounting the coils traveled on a segment of circular track, which was concentric with the flywheel. A pointer on the carriage indicated the angular position of the coils relative to engine top dead center. Measurement of θ_r consisted in moving the carriage until a timing mark coincided with the peak on the oscilloscope diagram, which indicated the maximum rate of pressure rise.

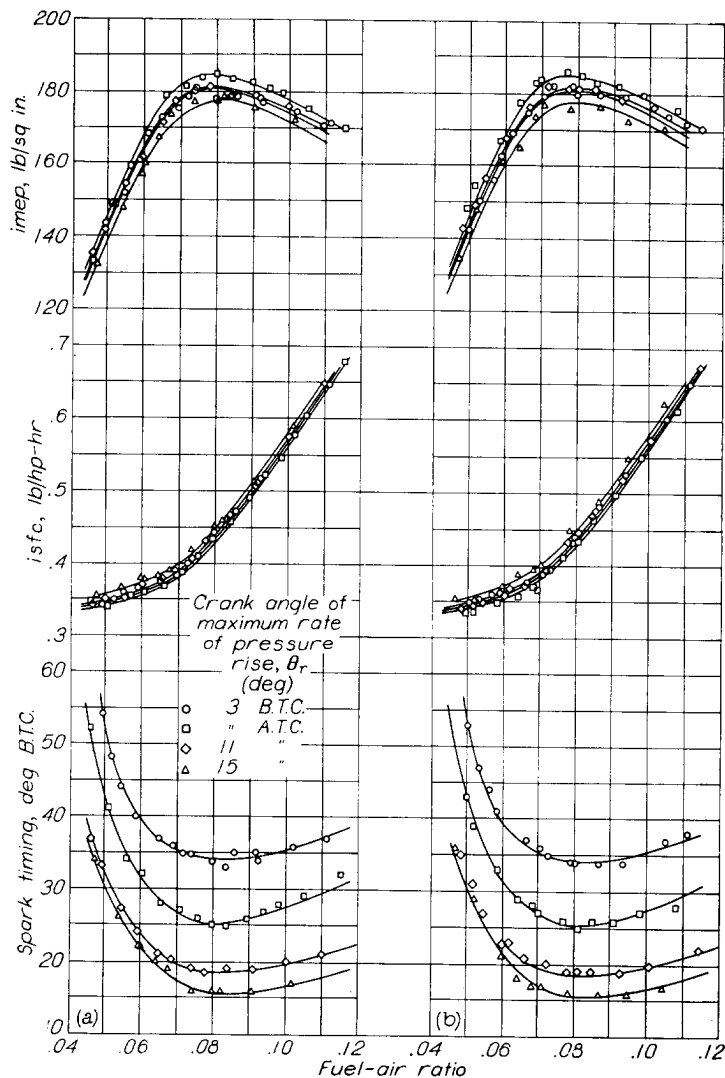
A spark-control instrument described in the appendix was used. The spark timing was manually controlled in runs where θ_r was held constant. Automatic control of spark timing was used in runs where the crank angle of passage of the flame front past an ionization gap was held constant.

The ionization gap consisted of a spark plug that was modified by extending the electrodes to form a gap 0.025 inch wide about $\frac{1}{8}$ inch inside the combustion chamber. When the ionization gap was used, the knock pickup was removed from the cylinder head and the modified spark plug was mounted in its place. The hole for mounting the knock pickup and the ionization gap was located in front of the cylinder midway between the front spark plug and the intake valve.

The ignition system for the engine was so connected that the magnetos for the front and rear spark plugs operated on one set of primary-circuit contact points. Therefore, the spark timing for the front and rear spark plugs was the same.

A series of variable fuel-air ratio, constant air-flow runs was conducted with the spark timing manually adjusted to maintain θ_r constant at 3° B. T. C., 3° A. T. C., 11° A. T. C.,

and 15° A. T. C. A second series of variable fuel-air ratio, constant air-flow runs was conducted with the spark-timing-control instrument set to maintain constant the crank angle at which the flame front passed the ionization gap. In the second series of runs, the instrument was set to give the same spark timings at a fuel-air ratio of 0.085 as were found in the first series of runs.



(a) Spark timing manually controlled for constant crank angle of maximum rate of pressure rise θ_r .

(b) Spark timing automatically controlled for constant crank angle of passage of flame front at ionization gap.

FIGURE 1.—Comparison of engine performance with spark timing manually controlled to maintain constant crank angle of maximum rate of pressure rise θ_r and with spark timing automatically controlled to maintain constant crank angle of passage of flame front at ionization gap. (Faired curves in figs. 1 (a) and 1 (b) are same. Runs of fig. 1 (b) were conducted with automatic spark-timing control set to give same spark timing at fuel-air ratio of 0.085 as was obtained in runs of fig. 1 (a).)

RESULTS AND DISCUSSION

Data obtained with spark timing manually controlled to maintain constant various crank angles of maximum rate of pressure rise are shown in figure 1 (a). Data obtained with automatically controlled spark timing to give constant crank angle of passage of the flame front by the ionization gap are shown in figure 1 (b). The curves of figures 1 (a) and 1 (b) are the same. The matching of the data obtained in the two series of runs shows that θ_r is constant when the crank angle of passage of the flame front by the ionization gap is constant. This result shows that a direct relation exists between θ_r and flame-front travel.

The relation of indicated specific fuel consumption to θ_r for various fuel-air ratios is shown in figure 2. (Data were extrapolated to include a fuel-air ratio of 0.04.) Lines of constant spark timing are also shown. Obviously, spark timing must be advanced to achieve the low indicated specific fuel consumptions that are possible with very lean mixtures. The data show that, for any fuel-air ratio, maximum-economy spark timing occurs when θ_r is 3° A. T. C. Because the spark-timing-control instrument can maintain θ_r constant at 3° A. T. C., the instrument can be used to maintain automatically maximum-economy spark timing when engine operating conditions are varied. This automatic control of spark timing can be used to advantage in conducting fuel or engine investigations.

Two engine operating variables that have a great effect on spark timing for maximum fuel economy are (1) the degree of dilution of the incoming charge by residual gases and (2) the use of internal coolants such as water. These variables were not included in this investigation; however, data in which the relation of exhaust pressure to inlet-air pressure was varied (reference 2) and unpublished data from investigations with various water-fuel ratios show that the relation of maximum-economy spark timing to θ_r of 3° A. T. C. is unaffected by these two variables. Data from reference 2 show that engine speed, compression ratio, and inlet-air temperature do not affect the relation. Even when operating with only one spark plug firing the same relation existed.

The percentage increase in fuel consumption when using constant spark timing or constant θ_r compared with operation at maximum-economy spark timing ($\theta_r = 3^\circ$ A. T. C.) is shown in figure 3. Constant spark-timing data show large variations in percentage increase in fuel consumption over the minimum obtainable at each fuel-air ratio. Operation at constant θ_r results in an almost constant percentage increase. For example, during operation with a θ_r of 11° A. T. C., the average percentage increase in fuel consumption was about 2 percent (varies from 1.4 to 2.4 percent) over the range of fuel-air ratios.

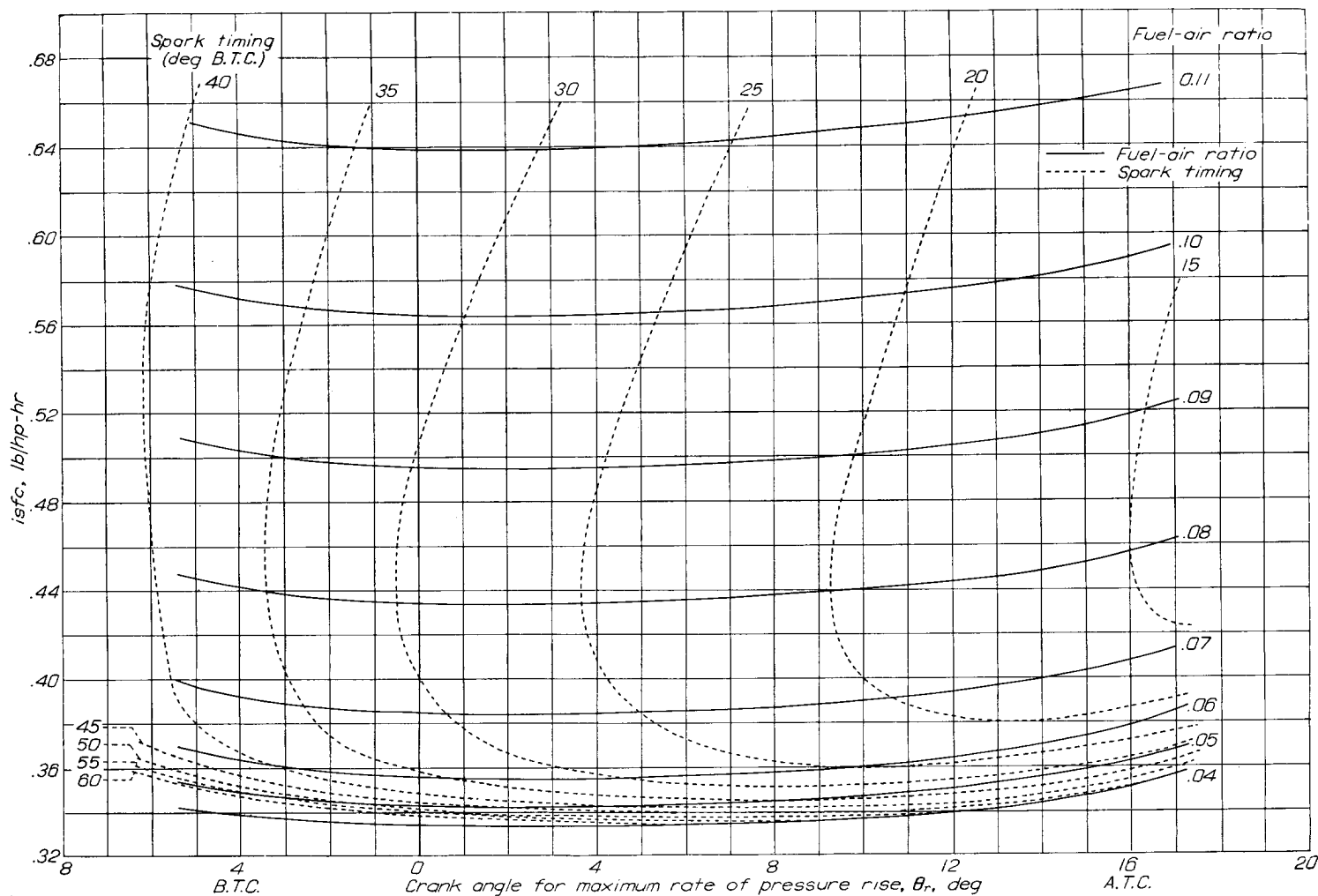


FIGURE 2.—Relation of indicated specific fuel consumption to crank angle of maximum rate of pressure rise θ_r for various fuel-air ratios and spark timings. (Cross plot from fig. 1.)

The spark-timing curves in figure 2 show that the time interval measured in degrees of crankshaft rotation between the spark timing and θ_r varied considerably. This variation in time (fig. 4) indicates changes in rate of flame-front travel or rate of combustion because there is a direct relation between θ_r and flame-front location.

For each fuel-air ratio, a spark timing exists that gives the maximum rate of combustion as indicated by the minimum time from spark timing to θ_r . The coincidence of this spark timing for maximum rate of combustion with the maximum-economy spark timing ($\theta_r = 3^\circ$ A. T. C.) for most of the range

of fuel-air ratios (0.06 to 0.10) is significant. The combined effect of maximum rate of combustion and proper timing of pressure rise appears to give maximum fuel economy. These results are consistent with theory in that maximum power should result with constant volume burning at top dead center.

The advance of the maximum-economy spark timing for lean mixtures (below 0.06) beyond the spark timing for minimum time from spark to θ_r is probably due to slow burning during initial stages of combustion caused by the low degree of compression of the charge.

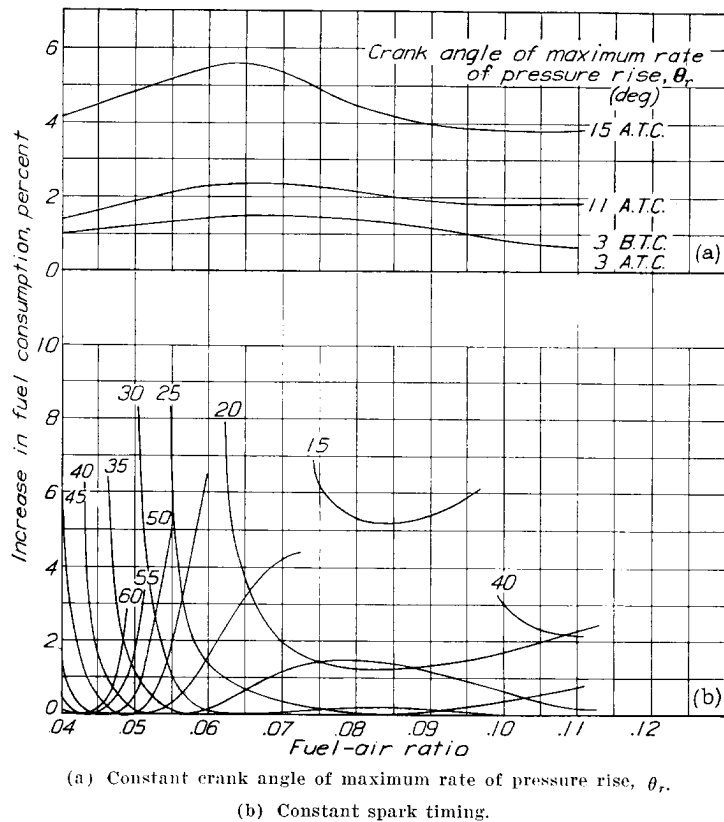


FIGURE 3.—Percentage increase in fuel consumption over that obtained with maximum-economy spark timing when fuel-air ratio is varied with various spark timings and crank angles of maximum rate of pressure rise θ_r . Numerical values indicate spark timing, degrees B.T.C. (Cross plot from fig. 2.)

APPLICATION OF RESULTS TO MULTICYLINDER-ENGINE OPERATION

The method for automatically controlling the spark timing to maintain constant θ_r as described for a single-cylinder engine can be applied to multicylinder engines. Magnetostriction knock pickups in the cylinder heads of a multicylinder engine, for example, could be used not only to indicate when knock occurs but also to trigger an instrument for automatically controlling θ_r . Then maximum-economy spark timing could be automatically maintained when the

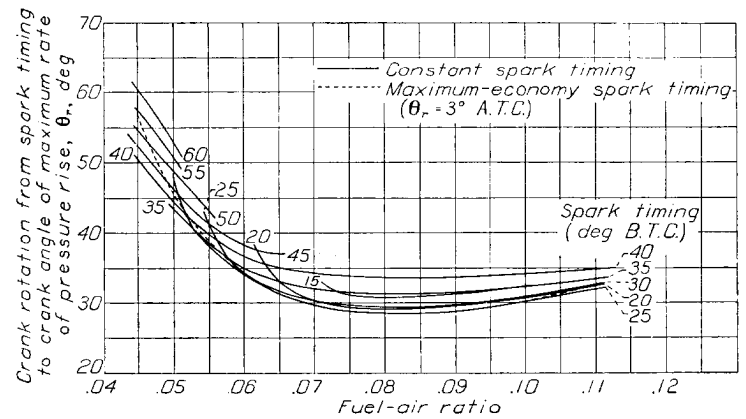


FIGURE 4.—Variation in crank rotation between spark timing and time of maximum rate of pressure rise with fuel-air ratio for constant spark timing and for maximum-economy spark timing. (Cross plot from fig. 2.)

fuel-air ratio or other engine operating conditions are varied. In addition, the same instrumentation could actuate a warning signal to indicate the occurrence of preignition.

SUMMARY OF RESULTS

The following results were obtained from experimental data on a full-scale air-cooled cylinder in the investigation of the relations between maximum-economy spark timing, flame-front travel, and cylinder-pressure rise:

1. Maximum-economy spark timing occurred when the crank angle of maximum rate of pressure rise was 3° A. T. C.
2. Maximum rate of pressure rise and the travel of the flame front were directly related.
3. For fuel-air ratios between 0.06 and 0.10, the highest rate of flame travel occurred when the crank angle of maximum rate of pressure rise was 3° A.T.C.
4. An instrument for controlling spark timing was developed that automatically maintained maximum-economy spark timing with varying engine operating conditions and indicated the occurrence of preignition.

AIRCRAFT ENGINE RESEARCH LABORATORY,
NATIONAL ADVISORY COMMITTEE FOR AERONAUTICS,
CLEVELAND, OHIO, November 22, 1946.

APPENDIX

DESCRIPTION OF SPARK-TIMING-CONTROL INSTRUMENT

The automatic spark-timing control (fig. 5) consists of two parts: The control unit, which contains the trigger circuit and amplifier, and the servo unit, which contains the magneto-breaker plate driven by a motor, a position transmitter, and limit switches.

The breaker plate is removed from the magneto and mounted on a shaft, which is alined with the magneto camshaft but is not coupled to it. The shaft on which the breaker

plate is mounted is driven by a two-phase induction motor through a worm gear and wheel with a reduction ratio of 100:1. The position transmitter is driven directly from the motor shaft through a spur gear with an over-all reduction ratio of 6:1. An arm on the breaker-plate shaft actuates limit switches at both extremes of travel of the breaker plate. The servo unit is bolted to the under side of the magneto mounting pad.

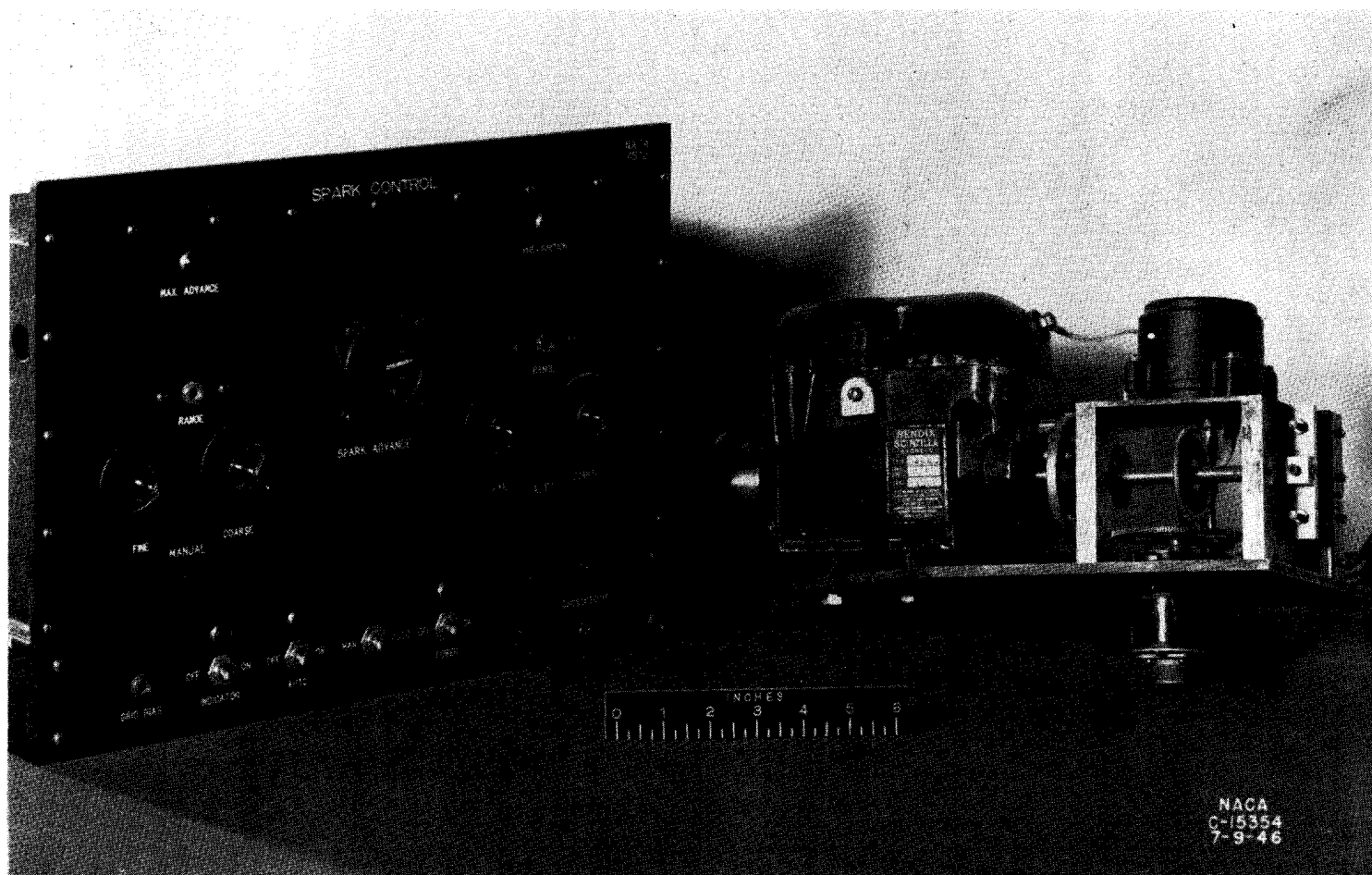


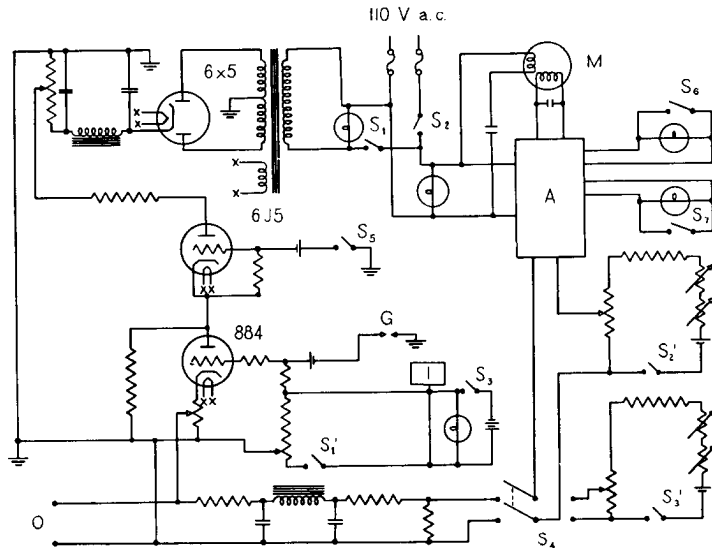
FIGURE 5.—Spark-timing-control instrument.

One phase of the motor is energized directly from a 110-volt alternating-current line. The second phase is energized by the output of a standard commercial amplifier, which utilizes a vibrator to convert a direct-current input signal to alternating current before amplification. A selector switch determines which of two available signals (manual or automatic) is to be fed to the amplifier. Both input signals are of the order of 10 millivolts direct current. A fixed “buck-

ing” voltage of the same order of magnitude, that is, 10 millivolts, opposes the input signal. When the input signal equals the bucking voltage, the amplifier output is zero; therefore, the motor is at rest and the system is at balance.

Manual control of spark timing is achieved by varying the manually controlled battery voltage above or below the bucking-voltage level until the desired spark timing is reached.

Automatic control of spark timing is achieved by means of a thyatron trigger circuit. The circuit (fig. 6) consists essentially of a vacuum tube (6J5, triode) in series with a thyatron (884). The thyatron is shunted with a 50,000-ohm resistor, which completes the series circuit through the triode when the thyatron is extinguished. In normal operation the thyatron is biased below its firing point. During the time of passage of the flame front, the ionization gap in the combustion chamber breaks down and applies a positive firing voltage on the grid of the thyatron allowing the thyatron to conduct current. An engine-driven switch set to close momentarily at about 100° A. T. C. applies a negative impulse to the grid of the triode driving it to cut-off, which breaks the circuit and extinguishes the thyatron. The triode conducts current as soon as the biasing switch opens and the circuit returns to normal operation.



A, Commercial amplifier with vibrator that converts direct-current input signal to alternating current

G, Ionization gap in combustion chamber

I, Indicator (position transmitter)

M, Two-phase induction motor designed to operate with commercial amplifier

O, Terminals for oscilloscope (used for testing operation of instrument)

Switches

S₁, Power to transformer

S₁', Grid bias voltage for thyatron (884), second circuit of double-pole switch

S₂, Power to amplifier and motor

S₂', Bridge circuit, second circuit of double-pole switch

S₃', Power to indicator and S₄'

S₃', Bridge circuit, second circuit of double-pole switch

S₄, Selector for automatic or manual control of spark timing

S₅, Engine-driven switch set to close momentarily at approximately 100° A. T. C.

S₆, Limit switch for maximum spark advance

S₆', Limit switch for minimum spark advance (indicates occurrence of pre-ignition)

FIGURE 6.—Electric circuit for spark-timing-control instrument.

Successive firing and extinguishing of the thyatron produces a square-wave voltage of constant amplitude across a 10,000-ohm resistor in the cathode circuit of the thyatron. The length of time during which the thyatron conducts current depends upon the point at which it is fired by the ionization gap; therefore, the width of the positive portion of the cycle is a function of the position of the maximum rate of pressure rise. The direct current that results from filtering the direct-current square wave is the second of the two signals that may be fed into the amplifiers.

The input polarity and the direction of rotation of the motor are such that as the ionization gap tends to break down sooner, the spark is retarded until the point of maximum rate of pressure rise returns to its original position and the system is rebalanced. Conversely, as the gap tends to break down later, the spark is advanced until balance is restored.

Limit switches so open the plate circuit of the proper power output tube of the amplifier that motor travel in either direction is restricted but the motor can reverse and travel in the opposite direction. These limit switches also control warning lights on the instrument panel. The warning light, which shows that the spark timing is fully retarded, can be used to indicate preignition of the engine.

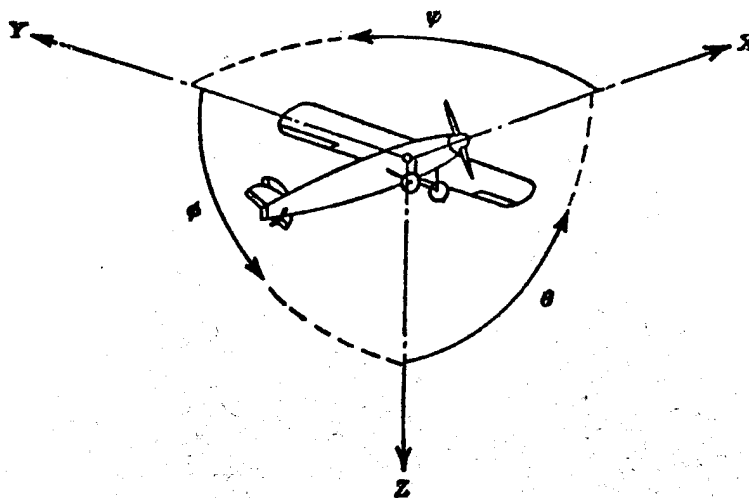
The functioning of the instrument as a preignition indicator is possible because when preignition occurs the crank angle of maximum rate of pressure rise θ_r is advanced considerably and the spark timing no longer controls the time of combustion. The instrument for controlling the spark timing therefore acts to retard the spark and proceeds to the limit of its travel. The reaching of this limit is indicated by the warning signal (a light marked "preignition" on the instrument, fig. 5).

Spark timing is shown on the instrument panel by the position indicator, which is electrically driven by the position transmitter geared to the motor shaft.

Originally the thyatron was to be triggered by the output of a magnetostriction-type knock pickup; however, this method was not used because it necessitated use of an additional amplifier. If the knock pickup were used, the instrument would be directly controlled by the crank angle of maximum rate of pressure rise.

REFERENCES

1. Cook, Harvey A., Held, Louis F., and Pritchard, Ernest I.: Comparison of Relative Sensitivities of the Knock Limits of Two Fuels to Six Engine Variables. NACA TN No. 1117, 1946.
2. Cook, Harvey A., and Brightwell, Virginia L.: Relation between Fuel Economy and Crank Angle for the Maximum Rate of Pressure Rise. NACA MR No. E5E21, 1945.



Positive directions of axes and angles (forces and moments) are shown by arrows

Axis		Force (parallel to axis) symbol	Moment about axis			Angle		Velocities	
Designation	Sym-bol		Designation	Sym-bol	Positive direction	Designa-tion	Sym-bol	Linear (compo-nent along axis)	Angular
Longitudinal.....	X	X	Rolling.....	L	Y→Z	Roll.....	ϕ	u	p r q
Lateral.....	Y	Y	Pitching.....	M	Z→X	Pitch.....	θ	v	
Normal.....	Z	Z	Yawing.....	N	X→Y	Yaw.....	ψ	w	

Absolute coefficients of moment

$$C_l = \frac{L}{q b S} \quad C_m = \frac{M}{q c S} \quad C_n = \frac{N}{q b S}$$

(rolling) (pitching) (yawing)

Angle of set of control surface (relative to neutral position), δ . (Indicate surface by proper subscript.)

4. PROPELLER SYMBOLS

D	Diameter	P	Power, absolute coefficient $C_p = \frac{P}{\rho n^3 D^5}$
p	Geometric pitch	C_s	Speed-power coefficient = $\sqrt{\frac{\rho V^6}{P n^3}}$
p/D	Pitch ratio	η	Efficiency
V'	Inflow velocity	n	Revolutions per second, rps
V_s	Slipstream velocity	ϕ	Effective helix angle = $\tan^{-1} \left(\frac{V}{2\pi r n} \right)$
T	Thrust, absolute coefficient $C_T = \frac{T}{\rho n^3 D^4}$		
Q	Torque, absolute coefficient $C_Q = \frac{Q}{\rho n^3 D^5}$		

5. NUMERICAL RELATIONS

1 hp = 76.04 kg-m/s = 550 ft-lb/sec
 1 metric horsepower = 0.9863 hp
 1 mph = 0.4470 mps
 1 mps = 2.2369 mph

1 lb = 0.4536 kg
 1 kg = 2.2046 lb
 1 mi = 1,609.35 m = 5,280 ft
 1 m = 3.2808 ft